Dynamics of a backlash chain

José A. Tenreiro Machado

Abstract: This paper studies the dynamical properties of a system with distributed backlash and impact phenomena. This means that it is considered a chain of masses that interact with each other solely by means of backlash and impact phenomena. It is observed the emergence of non-linear phenomena resembling those encountered in the Fermi-Pasta-Ulam problem.

PACS (2008): 05.45.-a, 05.10.-a, 79.20.Ap, 07.05.Tp

Keywords: backlash • impacts • nonlinear dynamics

1. Introduction

In 1953, at Los Alamos, Enrico Fermi, John Pasta, and Stan Ulam developed a pioneer study that is nowadays called the Fermi-Pasta-Ulam (FPU) problem. They simulated numerically a mechanical system composed of identical masses coupled by nonlinear springs, fixed a t the extreme points, using the computer MANIAC-1 (Mathematical Analyzer Numerical Integrator And Computer) [1]. Instead of using a linear model for the springs (i.e., the Hooke law) they adopted a nonlinear term, either quadratic (denoted FPU - α), or cubic (denoted FPU - β). Computer simulations revealed a complex quasi-periodic dynamics, considerably different from what linear systems would suggest. They expected that the energy introduced into the first m ode w ould d rift t o t he o ther m odes until reaching equipartition of energy. However, they verified t hat a lmost a ll e nergy w as b ack t o t he fi rst mode after some time and, moreover, a recurrence phenomenon, due the the occurrence of a kind of replicas of the initial state for longer periods of time [2–4]. The FPU experiment marked the beginning of computational physics and nonlinear science and triggered a huge volume of research during the last decades [5–23].

Vibration with impacts occurs in many areas of science and technology. In the context of mechanical engineering, backlash is due to clearance between adjacent movable parts as in gears. Its effect is visible when movement is reversed and contact is lost momentarily, being re-established later when mating components produce some form of impact [24–36]. This strong non-linearity is not yet fully understood due to the diversity of effects involved and the dynamical analysis and control of backlash is still an open issue.

Inspired by the FPU problem and the backlash nonlinearity, this paper embeds both concepts and investigates the dynamics of systems with chain of masses having backlash and impacts. Several relevant studies of lattices with

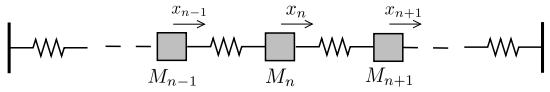

Figure 1. The FPU problem: a chain of N masses interconnected by springs.

hard collisions have been proposed during the last years [37–42]. The anomalous thermal conductivity was investigated, but this topic remains an important open area of research.

Bearing these ideas in mind, the present paper is organized as follows. Section 2 introduces the FPU problem and the dynamical description of backlash. Section 3 formulates a new problem, namely a chain of masses interconnected by means of backlash. The system is simulated and the dynamics of the distributed backlash chain of masses is analysed. Finally, section 4 draws the main conclusions.

2. Fundamental concepts

This section presents the main fundamental concepts applied in the sequel. Sub-section 2.1 formulates the classical FPU problem and sub-section 2.2 describes the dynamics of impacts.

2.1. The FPU dynamical system

The system formulated by Fermi, Pasta and Ulam consists of a chain of N masses interconnected by springs (Fig. 1). The equations of motion are:

$$\ddot{x}_n = (x_{n+1} - x_n) - (x_n - x_{n-1}) + K_s\left[(x_{n+1} - x_n)^p - (x_n - x_{n-1})^p\right] \quad (1)$$

where K_s is a parameter that reflects the strength of the nonlinearity and n, $1 \leq n \leq N$, is the index associated with each mass. The fixed extremes are represented by $n = 0$ and $n = N + 1$. When $p = 1$ it yields a linear model and when $p = 2$ (or $p = 3$) we have the FPU - α (or FPU - β) problem.

For the string k-th mode the sum of the kinetic and potential energies is given by:

$$E_k = \frac{1}{2}\left(\dot{A}_k^2 + \omega_k^2 A_k^2\right) \quad (2)$$

where A_k is related to the displacements by the expression:

$$A_k = \sqrt{\frac{2}{N+1}} \sum_{n=1}^{N} x_n \sin\left(\frac{nk\pi}{N+1}\right) \quad (3)$$

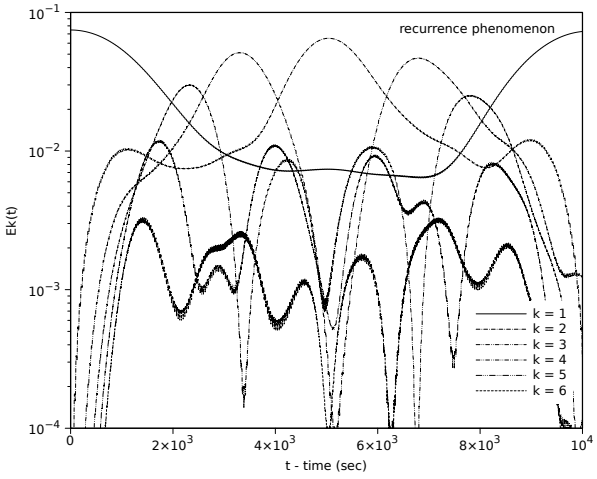

Figure 2. Time evolution of $E_k(t)$, $k = \{1, \cdots, 6\}$, and the FPU-α problem.

and frequencies:

$$\omega_k = 2\sin\left[\frac{k\pi}{2(N+1)}\right] \quad (4)$$

Figure 2 depicts a typical time evolution of $E_k(t)$, $k = \{1, \cdots, 6\}$, for the FPU-α, $K_s = 0.25$, for a period of time of 10^4 sec. During the simulations it is adopted a Runge-Kutta 4 numerical integration with time step $dt = 10^{-2}$ sec, $N = 32$ and the initial conditions formulated by Fermi, Pasta and Ulam, namely $x_n(0) = \sin\left(\frac{n\pi}{N+1}\right)$, $\dot{x}_n(0) = 0$. It is clearly visible the recurrence phenomenon.

2.2. Dynamic backlash

In this sub-section we consider the description of backlash by means of the impacts and the law of conservation of momentum. This approach gives the net change in velocity of each body and the energy exchange during collisions [43–47].

Let us consider the impact of two bodies along surfaces that are normal to the line connecting their centres of mass. In the so-called central impact the two bodies have velocity components only along this line and no rotational or sliding effects occur.

Figure 3 depicts a mechanical model consisting of two masses M_1 and M_2 with backlash Δ. Collision between the masses M_1 and M_2 occurs when $x_1 = x_2 - \frac{\Delta}{2}$ or $x_1 = x_2 + \frac{\Delta}{2}$. The velocities before the impact $\{\dot{x}_1, \dot{x}_2\}$ are related to the new values $\{\dot{x}_1', \dot{x}_2'\}$ by means of the empirical law:

$$\dot{x}_1' - \dot{x}_2' = -\varepsilon(\dot{x}_1 - \dot{x}_2),\ 0 \leq \varepsilon \leq 1. \quad (5)$$

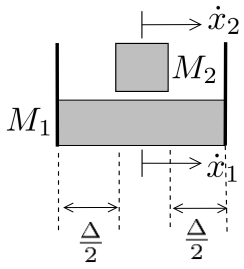

Figure 3. System with two masses M_1 and M_2 with velocities $\dot{x}_1$ and $\dot{x}_2$ with clearance Δ.

where ε denotes the coefficient of restitution that models the impact and t denotes time. The limit cases $\varepsilon = 0$ and $\varepsilon = 1$ consist of the fully plastic (or inelastic) and the ideal elastic collisions.

The principle of conservation of momentum requires that the momentum, immediately before and after the impact, is identical:

$$M_1\dot{x}_1' + M_2\dot{x}_2' = M_1\dot{x}_1 + M_2\dot{x}_2. \tag{6}$$

After combining equations (5)-(6) we get the velocities after impact:

$$\dot{x}_1' = \dot{x}_1\frac{M_1 - \varepsilon M_2}{M_1 + M_2} + \dot{x}_2\frac{(1+\varepsilon)M_2}{M_1 + M_2} \tag{7}$$

$$\dot{x}_2' = \dot{x}_1\frac{(1+\varepsilon)M_1}{M_1 + M_2} + \dot{x}_2\frac{M_2 - \varepsilon M_1}{M_1 + M_2}. \tag{8}$$

The energy loss E_L during impacts is given by:

$$E_L = \frac{(1-\varepsilon)^2}{2}\frac{M_1 M_2}{M_1 + M_2}\left(\dot{x}_1 - \dot{x}_2\right)^2. \tag{9}$$

3. A chain with backlash

In this section we consider the system represented in figure 4. This chain of N masses is inspired in the FPU problem, but the non-linear springs are now substituted by the backlash and impact phenomena. The symbols x_n and $\dot{x}_n$ denote the displacement and velocity of mass M_n, $n = 1, \ldots, N$ and $f(t)$ the input force, if any. In the chain each mass interacts with its left and right neighbours by means of impacts, with exception of the initial/final masses that have only one neighbour located at its right/left side. The parameters Δ and ε represent the backlash width and the coefficient of restitution, respectively. Therefore, while in the FPU system we are in the presence of non-dissipative elements, here such situation occurs only if $\varepsilon = 1$

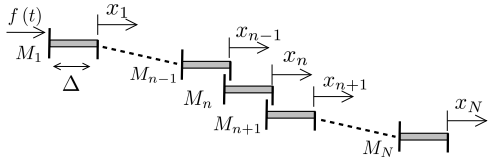

Figure 4. The chain of masses M_n, $n = 1, \ldots, N$, with displacement x_n, interconnected by backlash with clearance Δ.

Two distinct visualization methods are adopted, namely the time and the Fourier domain. In the first case is visualized the evolution of the energy $e_n(t) = \frac{1}{2}M_n\dot{x}_n^2$, $n = 1, \ldots, N$, along time t and in the second case is visualized the evolution of $|E_n(\omega)|$, $n = 1, \ldots, N$, along angular frequency ω, where $\mathcal{F}\{\cdot\}$ stands for the Fourier operator and $E_n(\omega) = \mathcal{F}\{e_n(t)\}$.

Since we are in the presence of a non-linear system the sets of initial conditions, input forces $f(t)$, parameters and their magnitudes have a large influence upon the final dynamical behaviour. In this line of thought, are considered four types of tests organized separately. In sub-section 3.1 is considered a sinusoidal input force with null initial conditions $f(t) = F\sin(\omega_0 t)$, $\{x_n(0), \dot{x}_n(0)\} = \{0, 0\}$. In sub-section 3.2 is analysed the case of random input force and null initial conditions, $f(t) = F \times random$, $\{x_n(0), \dot{x}_n(0)\} = \{0, 0\}$, where $random \in [0, 1]$. In sub-section 3.3 is addressed the case of null input force, null initial conditions in positions and Gaussian distributed initial velocities $f(t) = 0$, $\{x_n(0), \dot{x}_n(0)\} = \{0, \mathcal{N}(0, \sigma)\}$, where $\mathcal{N}$ denotes the Gaussian distribution and σ is the standard deviation. In sub-section 3.4 is studied null input force, null initial conditions in positions and velocities, with exception of the velocity in the middle mass $f(t) = 0$, $\{x_n(0), \dot{x}_n(0)\} = \{0, 0\}$, $n \neq \frac{N}{2}$, $\left\{x_{\frac{N}{2}}(0), \dot{x}_{\frac{N}{2}}(0)\right\} = \{0, \dot{x}_0\}$. Finally, in sub-section 3.5 is investigated the case of null input force, null initial conditions in positions and sinusoidal distributed initial velocities $f(t) = 0$, $x_n(0) = 0$ and $\dot{x}_n(0) = \dot{X}_0\sin\left(\frac{\pi n}{N}\right)$.

3.1. Sinusoidal input force and null initial conditions

We start by considering $f(t) = F\sin(\omega_0 t)$ and $\{x_n(0), \dot{x}_n(0)\} = \{0, 0\}$. Furthermore, is adopted $F = 0.1$, $\omega_0 = 1$ rad/s, $t \in [0, 5\cdot 10^3]$ sec, $\varepsilon = \{0.9, 1\}$, $\Delta = 0.1$ m and $N = 100$.

Figures 5 and 6 show $E_n(t)$ versus $\{t, n\}$ and $|E_n(\omega)|$ versus $\{\omega, n\}$, $n = 1, \ldots, N$, $\varepsilon = 1$, respectively. The time domain representation shows that some waves propagate along the chain. Furthermore, the total energy grows in time since we have a steady sinusoidal input

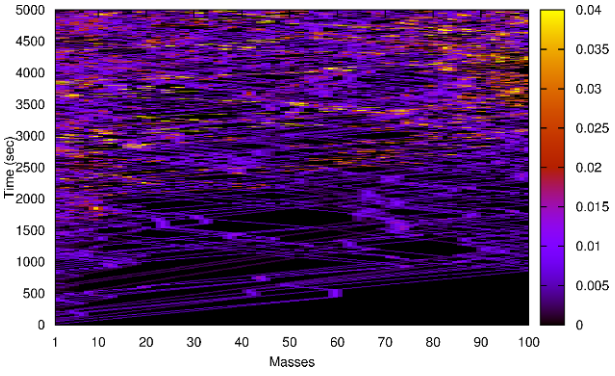

Figure 5. $E_n(t)$ versus $\{t, n\}$ for a chain of N masses interconnected by backlash ($\varepsilon = 1$) and $f(t) = F\sin(\omega_0 t)$.

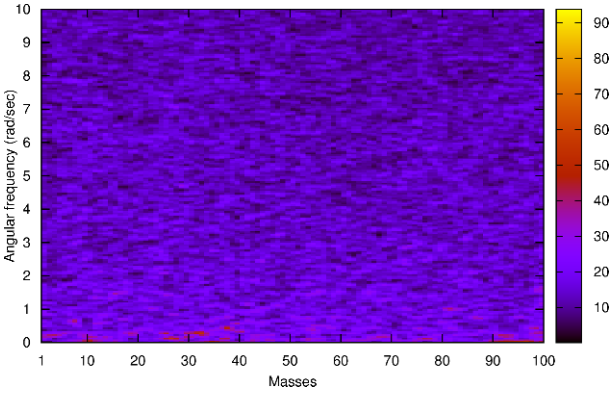

Figure 6. $|E_n(\omega)|$ versus $\{\omega, n\}$ for a chain of N masses interconnected by backlash ($\varepsilon = 1$) and $f(t) = F\sin(\omega_0 t)$.

$f(t) = F\sin(\omega_0 t)$. The frequency domain representation shows that we have an uniform distribution of the energy along all masses and a slight decay as ω increases. Figure 7 shows the total energy $E_t(t)$ in the chain versus time. We observe again that the total energy grows in time.

We now repeat the experiment for $\varepsilon = 0.9$. In this case energy dissipation occurs during impacts. Figures 8, 9 and 10 show $E_n(t)$, $|E_n(\omega)|$ and $E_t(t)$, respectively. We verify that the energy of the waves dissipates rapidly along the chain and that the total energy of the system settles at a low level with a noisy behaviour.

3.2. Random input force and null initial conditions

In this sub-section is analysed the case of random input force and null initial conditions, $f(t) = F \times random$, $\{x_n(0), \dot{x}_n(0)\} = \{0, 0\}$, where $random \in [0, 1]$. Furthermore, is adopted $F = 5000$, $t \in [0, 5\cdot 10^3]$ sec, $\varepsilon = 1$, $\Delta = 0.1$ m and $N = 100$.

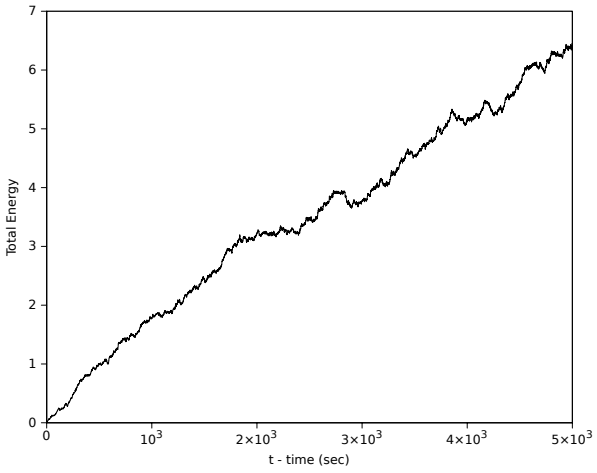

Figure 7. Total energy $E_t(t)$ for a chain of N masses interconnected by backlash ($\varepsilon = 1$) and $f(t) = F\sin(\omega_0 t)$.

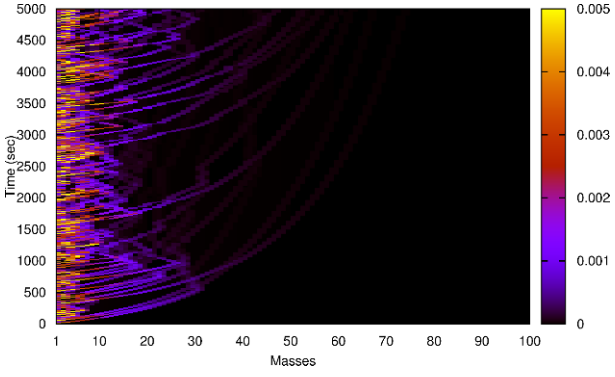

Figure 8. $E_n(t)$ versus $\{t, n\}$ for a chain of N masses interconnected by backlash ($\varepsilon = 0.9$) and $f(t) = F\sin(\omega_0 t)$.

Figures 11 and 12 show $E_n(t)$ versus $\{t, n\}$ and $|E_n(\omega)|$ versus $\{\omega, n\}$, $n = 1, \ldots, N$, $\varepsilon = 1$, respectively. The time and frequency domains shows that all masses are excited identically. Moreover, the energy grows with time since there is no dissipation.

3.3. Null input force, null initial conditions in positions and Gaussian distributed initial velocities

In this sub-section is addressed the case of null input force, null initial conditions in positions and Gaussian distributed initial velocities $f(t) = 0$, $\{x_n(0), \dot{x}_n(0)\} = \{0, \mathcal{N}(0, \sigma)\}$, where σ is the standard deviation. Furthermore, is adopted $\sigma = 100$, $t \in [0, 5\cdot 10^3]$ sec, $\varepsilon = 1$, $\Delta = 0.1$ m and $N = 100$.

Figures 13 and 14 show $E_n(t)$ versus $\{t, n\}$ and $|E_n(\omega)|$

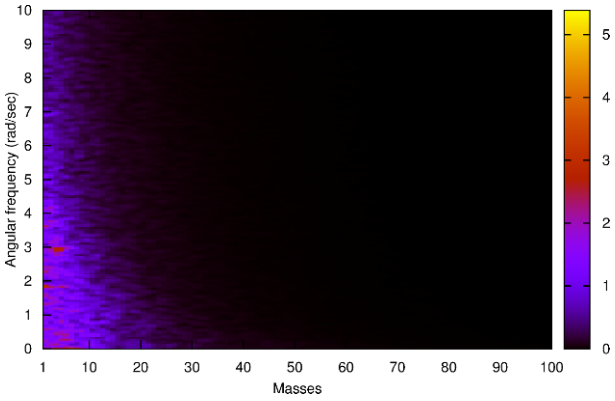

Figure 9. $|E_n(\omega)|$ versus $\{\omega, n\}$ for a chain of N masses interconnected by backlash ($\varepsilon = 0.9$) and $f(t) = F\sin(\omega_0 t)$.

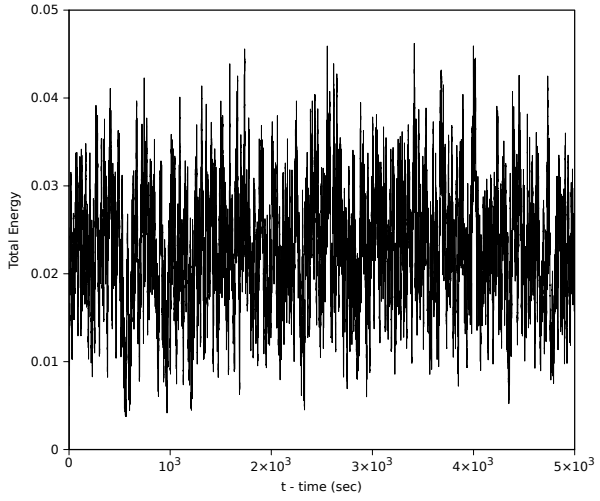

Figure 10. Total energy $E_t(t)$ for a chain of N masses interconnected by backlash ($\varepsilon = 0.9$) and $f(t) = F\sin(\omega_0 t)$.

versus $\{\omega, i\}$, $n = 1, \ldots, N$, $\varepsilon = 1$, respectively. The time and frequency domains shows that all masses have identical energy and that the total energy remains constant in time since there is neither input, nor dissipation.

3.4. Null input force and null initial conditions in positions and velocities, with exception of the velocity in the middle mass

In this sub-section is studied the case of null input force, null initial conditions in positions and velocities, with exception of the velocity in the middle mass $f(t) = 0$, $\{x_n(0), \dot{x}_n(0)\} = \{0, 0\}$, $n \neq \frac{N}{2}$, $\left\{x_{\frac{N}{2}}(0), \dot{x}_{\frac{N}{2}}(0)\right\} = \{0, \dot{x}_0\}$. Furthermore, is adopted $\dot{x}_{\frac{N}{2}}(0) = 0.1$, $t \in [0, 5\cdot 10^3]$ sec, $\varepsilon = 1$, $\Delta = 0.1$ m and $N = 100$.

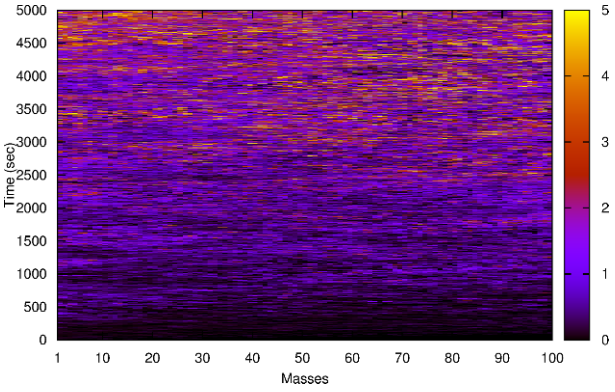

Figure 11. $E_n(t)$ versus $\{t, n\}$ for a chain of N masses interconnected by backlash ($\varepsilon = 1$) and $f(t) = F \times random$.

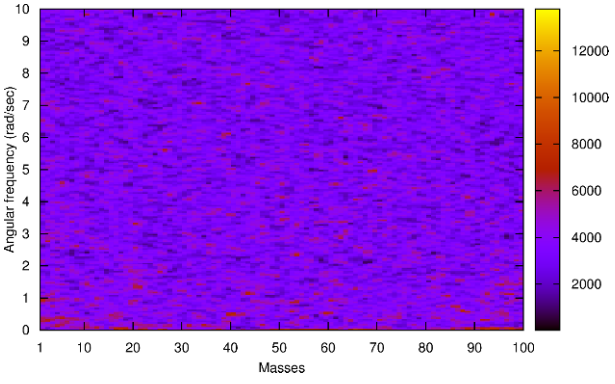

Figure 12. $|E_n(\omega)|$ versus $\{\omega, n\}$ for a chain of N masses interconnected by backlash ($\varepsilon = 1$) and $f(t) = F \times random$.

Figures 15 and 16 show $E_n(t)$ versus $\{t, n\}$ and $|E_n(\omega)|$ versus $\{\omega, i\}$, $n = 1, \ldots, N$, $\varepsilon = 1$, respectively. The time domain representation shows a constant velocity wave propagating along the chain that reflects at the terminal masses. The frequency domain representation shows that we have the signal energy concentrated at discrete harmonics.

3.5. Null input force, null initial conditions in positions and sinusoidal distributed initial velocities

In this sub-section is studied the case of null input force, null initial conditions in positions and sinusoidal distributed initial velocities $f(t) = 0$, $x_n(0) = 0$ and $\dot{x}_n(0) = \dot{X}_0 \sin\left(\frac{\pi n}{N}\right)$. Furthermore, is adopted $t \in [0, 5\cdot 10^3]$ sec, $\varepsilon = 1$, $\dot{X}_0 = 0.1$ m/s and $N = 100$.

Figures 17 and 18 show $E_n(t)$ versus $\{t, n\}$ and $|E_n(\omega)|$ versus $\{\omega, n\}$, $n = 1, \ldots, N$, $\varepsilon = 1$, respectively. The time domain representation shows a complex pattern of

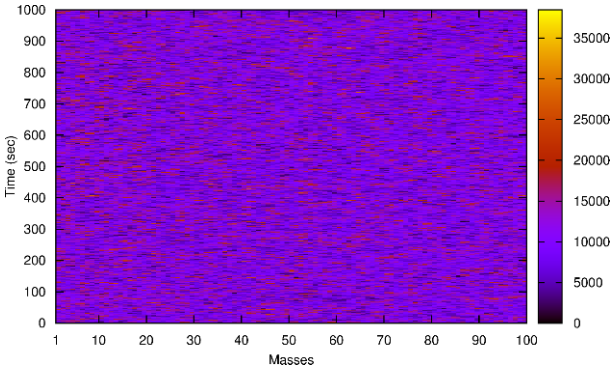

Figure 13. $E_n(t)$ versus $\{t, n\}$ for a chain of N masses interconnected by backlash ($\varepsilon = 1$) and $f(t) = F \times random$.

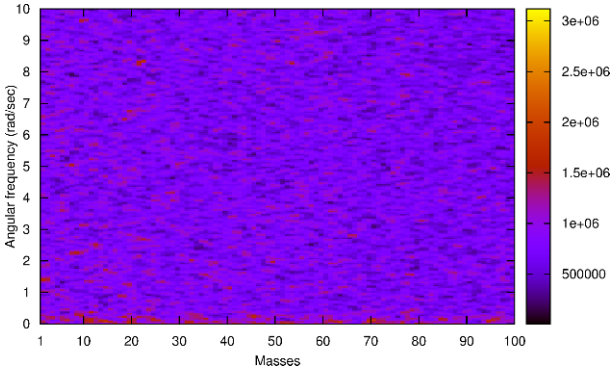

Figure 14. $|E_n(\omega)|$ versus $\{\omega, n\}$ for a chain of N masses interconnected by backlash ($\varepsilon = 1$) and $f(t) = F \times random$.

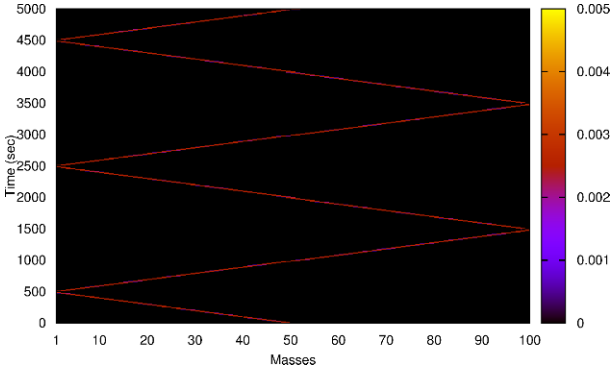

Figure 15. $E_n(t)$ versus $\{t, n\}$ for a chain of N masses interconnected by backlash ($\varepsilon = 1$) and $\left\{x_{\frac{N}{2}}(0), \dot{x}_{\frac{N}{2}}(0)\right\} = \{0, \dot{x}_0\}$.

wave propagating along time and space. The waves reflect at the terminal masses forming several smaller waves that interact between themselves. The frequency domain representation shows that we have the signal energy distribution mainly al low harmonics and that there is a fractal pattern although without depicting a net geometrical pattern.

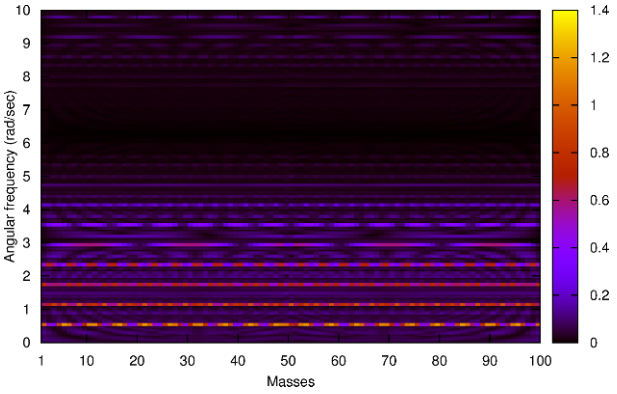

Figure 16. $|E_n(\omega)|$ versus $\{\omega, n\}$ for a chain of N masses interconnected by backlash ($\varepsilon = 1$) and $\left\{x_{\frac{N}{2}}(0), \dot{x}_{\frac{N}{2}}(0)\right\} = \{0, \dot{x}_0\}$.

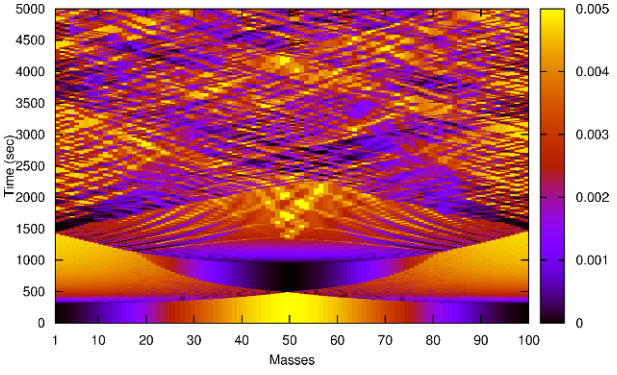

Figure 17. $E_n(t)$ versus $\{t, n\}$ for a chain of N masses interconnected by backlash ($\varepsilon = 1$) and $f(t) = 0$, $x_n(0) = 0$, $\dot{x}_n(0) = \dot{X}_0 \sin\left(\frac{\pi n}{N}\right)$.

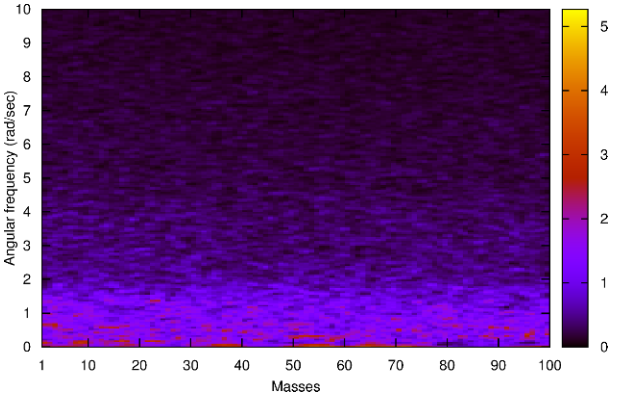

Figure 18. $|E_n(\omega)|$ versus $\{\omega, n\}$ for a chain of N masses interconnected by backlash ($\varepsilon = 1$) and $f(t) = 0$, $x_n(0) = 0$, $\dot{x}_n(0) = \dot{X}_0 \sin\left(\frac{\pi n}{N}\right)$.

4. Conclusions

In this paper was proposed a new system inspired in the Fermi-Pasta-Ulam problem. The non-linear system consists of a series of masses that interact dynamically with each other solely by means of backlash and impacts. The chain of masses was simulated numerically and the energy exchange was analysed both in the time and frequency domains. It was observed the emergence of several complex phenomena with some similarities to those discovered in the Fermi-Pasta-Ulam problem. This system provides new directions towards investigating the effect of non-linearities and backlash.

References

[1] E. Fermi, J. Pasta, S. Ulam, Studies of Nonlinear Problems, Los Alamos, LA-1940 (1955)
[2] J. Ford, Phys. Rep. 213, 271 (1992)
[3] T. P. Weissert, The Genesis of Simulation in Dynamics: Pursuing the Fermi-Pasta-Ulam Problem (Springer-Verlag, New York, 1997)
[4] M. A. Porter, N. J. Zabusky, B. Hu, D. K. Campbell, Am. Sci. 97, 214 (2009)
[5] D. J. Korteweg, G. de Vries, Philosophical Magazine 5th Series, 36, 422 (1895)
[6] N. J. Zabusky, M. D. Kruskal, Phys. Rev. Lett. 15, 240 (1965)
[7] F. M. Izrailev, B. V. Chirikov, Sov. Phys. Doklady 11, 30 (1966)
[8] N. J. Zabusky, G. S. Deem, J. Comput. Phys. 2, 126 (1967)
[9] P. Bocchieri, A. Scotti, B. Bearzi, A. Loinger, Phys. Rev. A 2, 2013 (1970)
[10] B. Chirikov, F. Izrailev, V. Tayurskij, Comput. Phys. Commun. 5, 11 (1973)
[11] R. Livi, M. Pettini, S. Ruffo, M. Sparpaglione, A. Vulpiani, Phys. Rev. A 31, 10395 (1985)
[12] M. Pettini, M. Landolfi, Phys. Rev. A 41, 768 (1990)
[13] J. De Luca, A. J. Lichtenberg, M. A. Lieberman, Chaos 5, 283 (1995)
[14] D. L. Shepelyansky, Nonlinearity 10, 1331 (1997)
[15] L. Casetti, M. Cerruti-Sola, M. Pettini, E. G. D. Cohen, Phys. Rev. E 55, 6566 (1997)
[16] S. Flach, C. R. Willis, Phys. Rep. 295, 181 (1998)
[17] G. James, Cr. Acad. Sci. II 332, 581 (2001)
[18] G. Benettin, Chaos 15, 015108 (2004)
[19] T. Dauxois, R. Khomeriki, F. Piazza, S. Ruffo, Chaos 15, 015110 (2005)
[20] T. Dauxois, M. Peyrard, S. Ruffo, Eur. J. Phys. 26, S3 (2005)
[21] S. Flach, M. V. Ivanchenko, O. I. Kanakov, Phys. Rev. E 73, 036618 (2006)
[22] D. Bambusi, A. Ponno, Commun. Math. Phys. 264, 539 (2006)
[23] T. Penati, S. Flach, Chaos 17, 023102 (2007)
[24] N. G. Dagalakis, D. R. Myers, The International Journal of Robotics Research 4, 65 (1985)
[25] Y. Stepanenko, T. S. Sankar, J. Dyn. Sys.-T. ASME 108, 9 (1986)
[26] Y. S. Choi, S. T. Noah, J. Dyn. Sys.-T. ASME 111, 253 (1989)
[27] J. L. Stein, C. Wang, Proc. American Control Conference, June 21-23, 2005, Seattle, Washington USA
[28] D. R. Seidl, S. Lam, J. A. Putman, R. D. Lorenz, IEEE T. Ind. Appl. 31, 1475 (1995)
[29] N. Sarkar, R. E. Ellis, T. N. Moore, Mechanical System and Signal Processing 11, 391 (1997)
[30] M. Nordin, P. Gutman, Proc. 39th IEEE Conf. on Decision and Control, Dec. 12-15, 2000, Sydney, Australia
[31] I. Trendafilova, H. Van Brussel, Mechanical System and Signal Processing 15, 1141 (2001)
[32] G. Hovland et al., Proc. of the 33rd Int. Symposium on Robotics, Oct. 7-11, Stockholm, Sweden
[33] M. Nordin, P. Gutman, Automatica 38, 1633 (2002)
[34] C. Su, M. Oya, H. Hong, IEEE T. Fuzzy Syst. 11, 1 (2003)
[35] C. Ma, Y. Hori, Proc. of American Control Conference, June 30-July 2, 2004, Boston, Massachusetts, USA
[36] R. Merzouki, J. A. Davila, J. C. Cadiou, L. Fridman, Proc. of American Control Conference, June 14-16, 2006, Minneapolis, Minnesota USA
[37] T. Prosen, M. Robnik, J. Phys. A Math. Gen. 25, 12, 3449 (1992)
[38] T. Prosen, D. K. Campbell, Chaos 15, 015117 (2005)
[39] L. Delfini, S. Lepri, R. Livi, A. Politi, Phys. Rev. E 73, 060201(R) (2006)
[40] L. Delfini, S. Denisov, S. Lepri, R. Livi, P. K. Mohanty, A. Politi, Eur. Phys. J. Spec. Top. 146, (2007)
[41] L. Delfini, S. Lepri, R. Livi, A. Politi, Phys. Rev. Lett. 100, 199401 (2008)
[42] A. Politi, J. Stat. Mech. Theory E. P03028 (2011)
[43] A. Azenha, J. T. Machado, Syst. Anal. Model. Sim. 33, 307 (1998)
[44] J. T. Machado, A. M. S. Galhano, J. Comput. Nonlin. Dyn. 3, 021201-1 (2008)
[45] F. Duarte, J. T. Machado, Nonlinear Dynam. 56, 409 (2009)
[46] M. F. M. Lima, J. T. Machado, M. Crisóstomo, Math. Comput. Model. 49, 1494 (2009)
[47] M. F. M. Lima, J. T. Machado, M. Crisóstomo, Robotica 29, 211 (2011)